Developmental Cell, Vol. 7, 697–707, November, 2004, Copyright ©2004 by Cell Press

FBF-1 and FBF-2 Regulate the Size of the Mitotic Region in the *C. elegans* Germline

Liana B. Lamont,[1] Sarah L. Crittenden,[2] David Bernstein,[1] Marvin Wickens,[1] and Judith Kimble[1,2,*]
[1]Department of Biochemistry
[2]Howard Hughes Medical Institute
University of Wisconsin-Madison
Madison, Wisconsin 53706

Summary

In the *C. elegans* germline, GLP-1/Notch signaling and two nearly identical RNA binding proteins, FBF-1 and FBF-2, promote proliferation. Here, we show that the *fbf-1* and *fbf-2* genes are largely redundant for promoting mitosis but that they have opposite roles in fine-tuning the size of the mitotic region. The mitotic region is smaller than normal in *fbf-1* mutants but larger than normal in *fbf-2* mutants. Consistent with gene-specific roles, *fbf-2* expression is limited to the distal germline, while *fbf-1* expression is broader. The *fbf-2* gene, but apparently not *fbf-1,* is controlled by GLP-1/Notch signaling, and the abundance of FBF-1 and FBF-2 proteins is limited by reciprocal 3′UTR repression. We propose that the divergent *fbf* genes and their regulatory subnetwork enable a precise control over size of the mitotic region. Therefore, *fbf-1* and *fbf-2* provide a paradigm for how recently duplicated genes can diverge to fine-tune patterning during animal development.

Introduction

The establishment of pattern is often coupled to growth and cell proliferation during animal development. Classic examples include the generation of somites as the vertebrate axis grows posteriorly (Pourquié, 2003), specification of distal-proximal pattern elements as the limb bud grows distally (reviewed in Tickle, 2003), and generation of plant lateral organs as the shoot apical meristem grows aerially (Carles and Fletcher, 2003). During this type of coupled growth and patterning, the tissue is polarized—cells at one pole are proliferative and remain in a relatively undifferentiated state, while cells at the other pole become incorporated into the maturing pattern element and begin to differentiate. A similar situation persists into adulthood in some tissues, where stem cells reside in one area, presumably near a stem cell niche, and cells begin to differentiate as they move out of the niche (reviewed in Fuchs et al., 2004).

The *C. elegans* germline provides a genetically tractable model for analysis of the mechanisms that couple growth and differentiation to generate pattern. This paper focuses on understanding controls of the size of the germline "mitotic region," which includes germline stem cells. Germ cells switch from the mitotic cell cycle into the meiotic cell cycle as they progress from the mitotic region into the "transition zone" (TZ), where they enter early meiotic prophase. The boundary between the mitotic region and transition zone is defined operationally as the position where mitotic divisions cease and most germline nuclei have entered early meiotic prophase. The polarity of the germline is controlled by the distal tip cell (DTC), which uses GLP-1/Notch signaling to stimulate proliferation (reviewed in Crittenden et al., 2003). In adults, the DTC serves as a stem cell niche: it is both necessary and sufficient to promote germline mitoses when downstream regulators are intact. The DTC signals to the germline using the LAG-2/Delta ligand, and germ cells respond using the GLP-1/Notch receptor. In the absence of either DTC or GLP-1/Notch signaling, germ cells that would normally be in the mitotic cell cycle instead enter meiotic prophase and undergo gametogenesis. The target genes activated by GLP-1/Notch signaling to control germline mitoses have remained elusive.

In addition to GLP-1/Notch signaling, RNA binding proteins are key regulators of the germline decision between proliferation and differentiation. Of particular importance to this paper are FBF-1 and FBF-2 (for *fem-3* Binding Factor), two nearly identical regulators of the PUF (Pumilio and FBF) protein family (Wickens et al., 2002; Zhang et al., 1997). The FBF-1 and FBF-2 proteins are collectively called FBF, and similarly, *fbf-1* and *fbf-2* are collectively called the *fbf* genes. The nucleotide sequences of *fbf-1* and *fbf-2* are 93% identical, and the amino acid sequences are 91% identical, suggesting that *fbf-1* and *fbf-2* are recently duplicated genes (Zhang et al., 1997). During early larval stages, germline proliferation is normal in *fbf-1 fbf-2* double mutants, but in the fourth larval stage (L4), the germline precociously leaves the mitotic cell cycle to enter meiosis and differentiate as sperm (Crittenden et al., 2002). In addition, depletion of both *fbf-1* and *fbf-2* eliminates the hermaphrodite switch from spermatogenesis to oogenesis (Zhang et al., 1997). Therefore, FBF is required for continued mitotic divisions in the germline as well as for the hermaphrodite sperm/oocyte switch.

PUF proteins bind specifically to regulatory elements, usually in the 3′ untranslated region (UTR) of a target mRNA, and repress that mRNA—either by promoting mRNA degradation or inhibiting translation (Wickens et al., 2002). Pumilio, for example, inhibits translation of *hunchback* mRNA in the early *Drosophila* embryo (Murata and Wharton, 1995), whereas PUF-5/Mpt5 destabilizes *HO* mRNA in yeast (Tadauchi et al., 2001). In *C. elegans*, FBF-1 and FBF-2 promote mitosis by repressing mRNAs that encode regulators critical for entry into the meiotic cell cycle (Crittenden et al., 2002; Eckmann et al., 2004), and they promote the sperm/oocyte switch by repressing the *fem-3* sperm-promoting mRNA (Zhang et al., 1997). Both FBF-1 and FBF-2 bind specifically to the same RNA target sequence, which differs from the Pumilio binding site (Crittenden et al., 2002; Eckmann et al., 2004; Zhang et al., 1997). The molecular mechanism by which FBF represses mRNAs in the *C. elegans* germline remains unknown, but by analogy

*Correspondence: jekimble@facstaff.wisc.edu

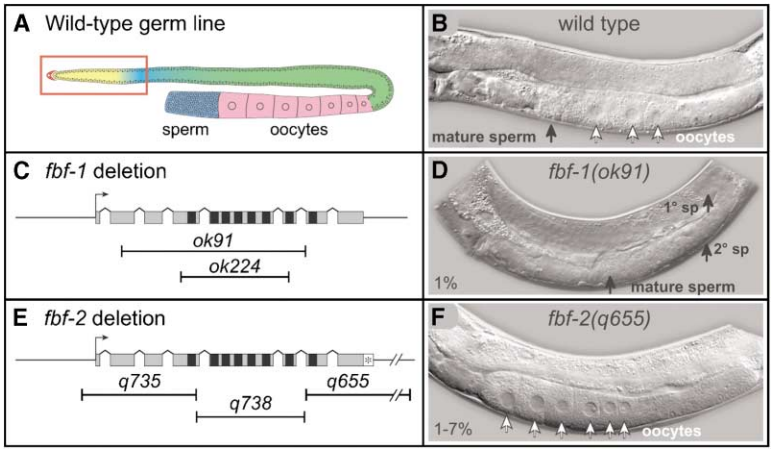

Figure 1. *fbf-1* and *fbf-2* Single Mutants Have Minor, but Opposite, Sperm/Oocyte Defects

(A) Organization of adult hermaphrodite germline. Sperm and oocytes are made in the proximal arm of a U-shaped germline. The distal end (boxed in red) includes the mitotic region (yellow), transition zone (light blue), and germ cells arrested in meiotic pachytene (green).

(B) Wild-type adult hermaphrodite germline, Nomarski micrograph.

(C) Top, the *fbf-1* gene. Exons, boxes; introns, lines; PUF repeats, black. Bottom, extent of two *fbf-1* deletions.

(D) Rare (~1%) *fbf-1* single mutants are sterile and masculinized, making many more sperm than normal. Black arrows highlight primary spermatocytes, secondary spermatocytes, and mature sperm.

(E) Top, the *fbf-2* gene. Same conventions as in (C), except asterisk represents the novel C-terminal FBF-2 region. Bottom, extent of three *fbf-2* deletions.

(F) Rare (1%–7%, depending on allele) *fbf-2* single mutants are self-sterile and feminized; the spermatheca is empty and only oocytes are produced. These "females" can produce cross-progeny if mated.

with its homologs in yeast and *Drosophila*, FBF is likely to control the stability or translation of its target mRNAs.

Previous studies suggested that FBF-1 and FBF-2 are redundant: *fbf-1* single mutants are grossly normal, albeit with smaller mitotic regions and more hermaphrodite sperm than wild-type (Crittenden et al., 2002). In this paper, we confirm the *fbf-1*/*fbf-2* redundancy but also identify individual roles for each gene in regulating the size of the mitotic region. Like *fbf-1*, the *fbf-2* single mutants are grossly normal, but in contrast to *fbf-1*, *fbf-2* mutant germlines have a larger mitotic region than normal and can be feminized. Consistent with *fbf-1* and *fbf-2* having individual roles, we find that their mRNAs and proteins are expressed in distinct patterns. Furthermore, the *fbf-2* gene appears to be a direct target of GLP-1/Notch signaling, a finding that forges the first molecular link between GLP-1/Notch signaling and the RNA regulatory circuit. We find that *fbf-1* and *fbf-2* repress each other's expression and that this reciprocal repression is likely to be direct via FBF binding sites in the *fbf-1* and *fbf-2* 3′ UTRs. We suggest that GLP-1/Notch signaling and FBF autoregulation work together to control the distribution and amount of FBF and thereby fine-tune the size of the mitotic region.

Results

fbf-1 and *fbf-2* Mutants

Wild-type hermaphrodites make ~300 sperm (~150 in each of two arms) and then switch into oogenesis (Figures 1A and 1B). Similarly, *fbf-1* null mutants (Figure 1C) make both gametes, although they make more sperm than normal (Crittenden et al., 2002). Indeed, rare *fbf-1* mutant hermaphrodites are sterile, making many more sperm than normal and failing to switch into oogenesis (Figure 1D).

To examine the *fbf-2* phenotype, we generated three *fbf-2* deletion mutants, each with a different region of the gene removed (Figure 1E). The *fbf-2(q735)* allele deletes 1052 bp, including the initiation codon and sequences encoding the N-terminal PUF repeat; *fbf-2(q738)* deletes 1084 bp, including sequences encoding six of the eight PUF repeats; *fbf-2(q655)* deletes 1400 bp, including the C-terminal PUF repeat and Csp domain. By RT-PCR, *fbf-2* mRNA was not detected in *fbf-2(q735)* mutants, but it was detected in *fbf-2(q655)* and *fbf-2(q738)* mutants; the RT-PCR products confirmed the latter two deletions and revealed a frameshift leading to premature termination for *fbf-2(q738)*. By immunocytochemistry, FBF-2 protein was not detected in *fbf-2(q655, q735*, or *q738)* homozygotes (see below). Because all PUF repeats are required for RNA binding (Wickens et al., 2002) and because all three *fbf-2* alleles have essentially the same phenotype (see below), they are likely all strong loss-of-function or null alleles.

Most *fbf-2* single mutant hermaphrodites are self-fertile (*q735*, 98%, n = 941; *q738*, 98%, n = 2201; *q655*, 91%, n = 1630). Therefore, the *fbf-2* gene, like *fbf-1*, is not essential for germline development. However, *fbf-2* XX germlines were sometimes feminized, possessing no cells typical of spermatogenesis (Figure 1F) (*q735*, 1%, n = 941; *q738*, 1%, n = 2201; *q655*, 7%, n = 1630). We conclude that *fbf-1* and *fbf-2* are essentially redundant to each other but that they have reproducible and opposite effects on germline sex determination.

fbf-1 and *fbf-2* Mutants Have Opposite Effects on Size of Mitotic Region

In wild-type germlines, the mitotic region contains ~250 germ cells and extends ~19 germ cell diameters from the distal end (Figures 2A, 2B, and 4H; Crittenden et al., 1994; Eckmann et al., 2004; Hansen et al., 2004). In contrast, *fbf-1* mitotic regions were shorter and had fewer total germ cells (Figures 2C and 4H; also see Crittenden et al., 2002), and *fbf-2* mitotic regions were longer and had more germ cells (Figures 2D and 4H). Indeed, the mitotic region of *fbf-2* germlines contained ~400 germ cells on average, and it extended ~27 germ cell diameters from the distal tip. To corroborate these size changes visualized by DAPI staining, we examined the positions of anti-PH3 (phosphorylated histone H3)-positive nuclei in *fbf-1* and *fbf-2* single mutant germlines. Consistent with the DAPI result, the range of anti-PH3-positive nuclei was shorter than normal in *fbf-1* mutants

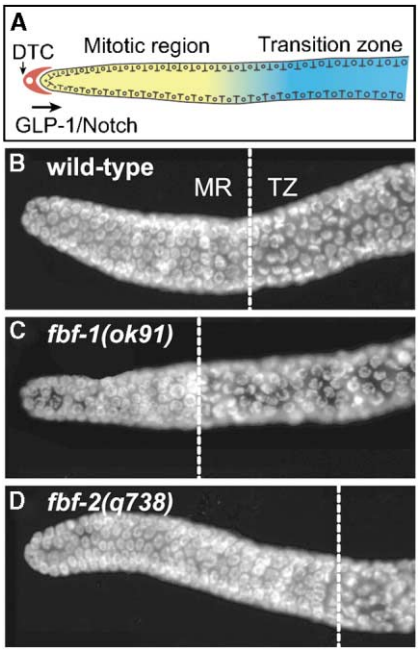

Figure 2. *fbf-1* and *fbf-2* Single Mutants Have Opposite Effects on the Size of the Germline Mitotic Region

(A) Germline distal end. DTC, distal tip cell; MR, mitotic region; TZ, transition zone.

(B–D) Extruded adult hermaphrodite germlines, DAPI-stained; distal end to left. Dashed line, MR/TZ boundary as defined in the text.

(B) Wild-type.

(C) *fbf-1(ok91)* homozygote.

(D) *fbf-2(q738)* homozygote.

and longer in *fbf-2* mutants (Figure 4H). Furthermore, two other markers of the mitotic region, GLP-1 and REC-8, were similarly affected (not shown). We conclude that *fbf-1* and *fbf-2* have reproducible and opposite effects on the size of the mitotic region.

Distinct Patterns of *fbf-1* and *fbf-2* mRNAs

The *fbf-1* and *fbf-2* phenotypic differences might reflect gene-specific regulation. We therefore examined their mRNAs by in situ hybridization. The *fbf-1* and *fbf-2* mRNA transcripts are 90.4% identical across their length, making it difficult to examine each transcript individually in wild-type germlines. To circumvent this technical obstacle, we designed an 841 nt hybridization probe that recognizes a sequence in the middle of both genes and that is deleted in the *fbf-1(ok91)* and *fbf-2(q738)* single mutants. In wild-type germlines, the antisense, but not the sense, probe detected RNAs broadly distributed in the distal germline (Figures 3A and 3B). To examine *fbf-1* mRNA specifically, we hybridized dissected *fbf-2(q738)* germlines and found staining with the antisense probe throughout the distal arm (Figure 3C). To examine *fbf-2* mRNA specifically, we hybridized dissected *fbf-1(ok91)* germlines and found staining with the antisense probe that was most abundant in the distal end (Figure 3D). Because these experiments had to be done in *fbf* single mutants, the mRNA distributions may not be identical to that of wild-type germlines. We conclude, therefore, that *fbf-1* and *fbf-2* mRNAs are present in distinct patterns.

Distinct Patterns of FBF-1 and FBF-2 Proteins

To examine FBF-1 and FBF-2 proteins individually, we used antibodies that specifically recognize each protein. As reported previously (Crittenden et al., 2002), FBF-1-specific antibodies stain weakly in the most distal mitotic nuclei of wild-type germlines and more strongly in the proximal three-fourths of the mitotic region. Strong FBF-1 staining begins ~6 germ cell diameters from the distal tip and extends to ~20 germ cell diameters (Figures 4A and 4H). The FBF-1 protein distribution in wild-type germlines is consistent with the broad distribution of *fbf-1* mRNA observed in *fbf-2* mutants.

To detect FBF-2 specifically, we raised a polyclonal antibody against the FBF-2-specific C-terminal extension (asterisk, Figure 1E). This antibody recognized recombinant FBF-2 on Western blots, but not FBF-1 or PUF-8, another *C. elegans* PUF protein (Figures 4C and 4D). By immunocytochemistry, FBF-2 staining was faint, but reproducible, in germ cells directly adjacent to the distal tip cell, extending proximally ~17 germ cell diameters (Figures 4E and 4H). The FBF-2 antibody did not detect protein in *fbf-2(q738), fbf-2(q655)*, or *fbf-2(q735)* germlines (Figure 4F; not shown) and, therefore, it is specific. The distal FBF-2 protein distribution in wild-type germlines is consistent with the distal *fbf-2* mRNA distribution observed in *fbf-1* mutants. We conclude that FBF-1 and FBF-2 overlap throughout most of the mitotic region but that FBF-1 appears to extend farther proximally than FBF-2.

FBF-1/FBF-2 Reciprocal Repression

We next examined FBF-1 and FBF-2 proteins in *fbf-2* or *fbf-1* single mutants, respectively. In *fbf-2* mutant germlines, FBF-1 protein increased in both level and extent compared to wild-type (Figures 4A and 4B). A similar increase in FBF-1 abundance was seen in all three *fbf-2* mutants (*q655*, *q735*, and *q738*). Strong anti-FBF-1 staining was sometimes visible all the way to the distal end, but more typically it extended ~5–29 germ cell diameters along the distal-proximal axis from the DTC (Figures 4B and 4H). In the converse experiment, FBF-2 was more abundant in *fbf-1* mutants than wild-type, but its extent was not dramatically increased (Figures 4E and 4G). Strong FBF-2 staining began adjacent to the DTC and remained strong until ~18 germ cell diameters from the DTC (Figure 4H). We conclude that FBF-1 and FBF-2 protein levels are sensitive to the presence or absence of the other FBF.

To ask whether FBF-1 and FBF-2 might regulate their own expression directly, we examined their 3′ UTRs for putative FBF binding elements (FBEs). Using a consensus sequence for FBF binding (see Experimental Procedures), we identified three potential FBEs in both *fbf-1* and *fbf-2* 3′ UTRs (Figure 5A). All candidate sites carry the crucial UGUR motif invariably present in PUF binding sites (Figure 5C). We refer to potential sites in the *fbf-1* 3′ UTR as FBE-1x and to specific sites in *fbf-2* as FBE-2x; the FBE-1a and FBE-2a sites are identical and are called FBE-a for simplicity.

To assay FBF binding to each candidate FBE, we used the yeast three-hybrid system (Figure 5B; Bernstein et al., 2002; SenGupta et al., 1996). Briefly, a LexA/MS2 fusion protein tethers a hybrid RNA (MS2 RNA plus candidate FBE) to a promoter in yeast. A second plasmid,

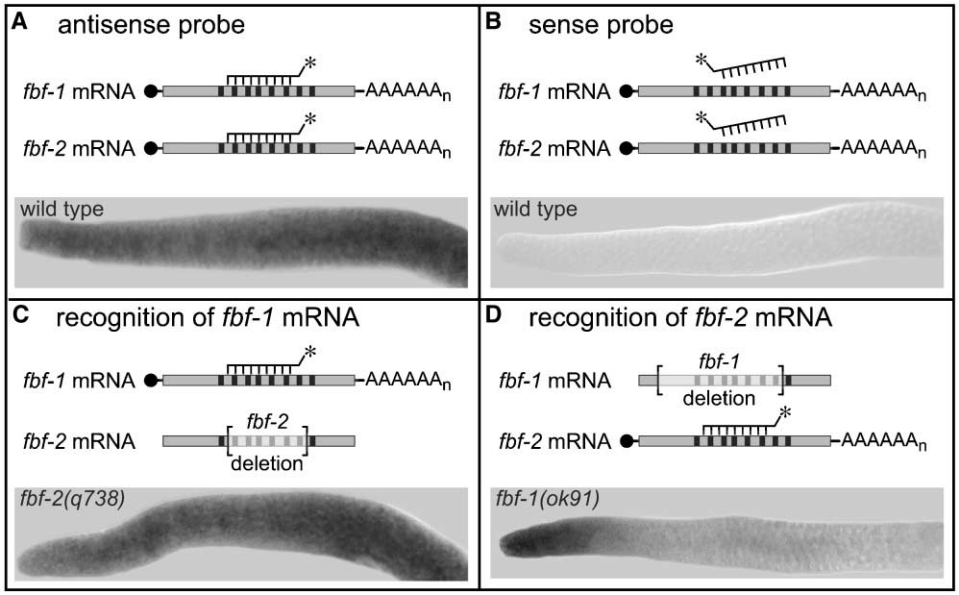

Figure 3. *fbf-1* and *fbf-2* mRNAs Are Expressed in Distinct Patterns

Top, hybridization probe detects a region 96% identical in *fbf-1* and *fbf-2* mRNAs. Bottom, extruded adult germline; distal end to left. Asterisk represents the digoxygenin-labeled probe.

(A) Wild-type germline, hybridized with antisense probe.

(B) Wild-type germline, hybridized with sense probe.

(C) *fbf-2(q738)* single mutant germline, hybridized with antisense probe. Only *fbf-1* mRNA can be detected.

(D) *fbf-1(ok91)* single mutant germline, hybridized with antisense probe. Only *fbf-2* mRNA can be detected.

carrying either FBF-1 or FBF-2 fused to a transcription activation domain (FBF/AD), was introduced into the same strain, and binding was monitored by activation of *LacZ* and *HIS3* reporters. By this method, both FBF-1 and FBF-2 bound to FBE-a, the identical sequence in both *fbf* 3′ UTRs (Figure 5C). Binding to FBE-a was specific, in that it required the UGU motif and was not detected with a different *C. elegans* PUF protein, PUF-5 (Figure 5C). FBF-2 also bound weakly to FBE-1b, but not to FBE-2b (Figure 5C). Neither FBF-1 nor FBF-2 bound to any other candidate FBEs.

To determine whether FBF binds FBE-a in the absence of other factors, we used purified, recombinant FBF-2 and RNAs containing the FBE-a sequence (Figure 5C). Using a gel electrophoretic mobility shift assay, FBF-2 bound the FBE-a RNA (Figure 5D). Binding was specific, since it was eliminated by changing the UGU to ACA (Figure 5D). We conclude that FBF-1 and FBF-2 bind specifically and directly to an FBE in each of the *fbf-1* and *fbf-2* 3′ UTRs.

LAG-1 Binding Sites in the *fbf-2* 5′ Flanking Region

The *fbf-2* mRNA and protein are both enriched in the distal germline (Figures 3D, 4E, and 4G). This distribution suggests that the DTC and GLP-1/Notch signaling might control *fbf-2* expression. To ask if *fbf-2* might be a direct transcriptional target of GLP-1 signaling, we first examined its genomic sequence for potential LAG-1 binding sites. LAG-1 is the sequence-specific DNA binding protein that responds to LIN-12 and GLP-1 (both Notch receptors) signaling; LAG-1 binds the consensus site RTGRGAA (Christensen et al., 1996), which occurs in regulatory regions of LIN-12 target genes (Berset et al., 2001; Yoo et al., 2004). Based on bioinformatic analyses, two other sequence motifs, motifs 1 and 2, are predicted to occur within 2 kb of consensus LAG-1 binding site clusters (Yoo et al., 2004; Yu et al., 2004).

Inspection of the *fbf-2* genomic sequence revealed four consensus LAG-1 binding sites (LBS-1–LBS-4) in the 5′ flanking region; motifs 1 and 2 are also present (Figures 6A, top, and 6B). By contrast, the *fbf-1* 5′ flanking region harbored no LAG-1 consensus binding sites, although one divergent site (*) was present in the region corresponding to *fbf-2* LBS-1 (Figures 6A, bottom, and 6B). We used a gel electrophoretic mobility shift assay to test if LAG-1 binds to all four consensus *fbf-2* LBS sites as well as the divergent *fbf-1* site. All four sites in the *fbf-2* 5′ flanking region bound purified LAG-1 (Figure 6C, left; data not shown), but the divergent *fbf-1** site did not bind well (Figure 6C, right). To test specificity of the LBS-1/LAG-1 binding, we used unlabeled LBS-1 or *fbf-1** as competitors (Figure 6D). Unlabeled *fbf-1** DNA did not compete with LAG-1 binding to ^{32}P-labeled LBS-1, but unlabeled *fbf-2* LBS-1 DNA did compete with binding. We conclude that LAG-1 binds in vitro to elements in the 5′ flanking region of the *fbf-2* gene.

fbf-2 Expression Responds to GLP-1 Signaling In Vivo

To test the *fbf-2* 5′ flanking DNA for its ability to drive transcription in vivo, we first attempted to make reporter transgenes driving GFP; however, GFP expression was not detectable (not shown). In parallel experiments with tagged *fbf* transgenes, mutant rescue was obtained, but

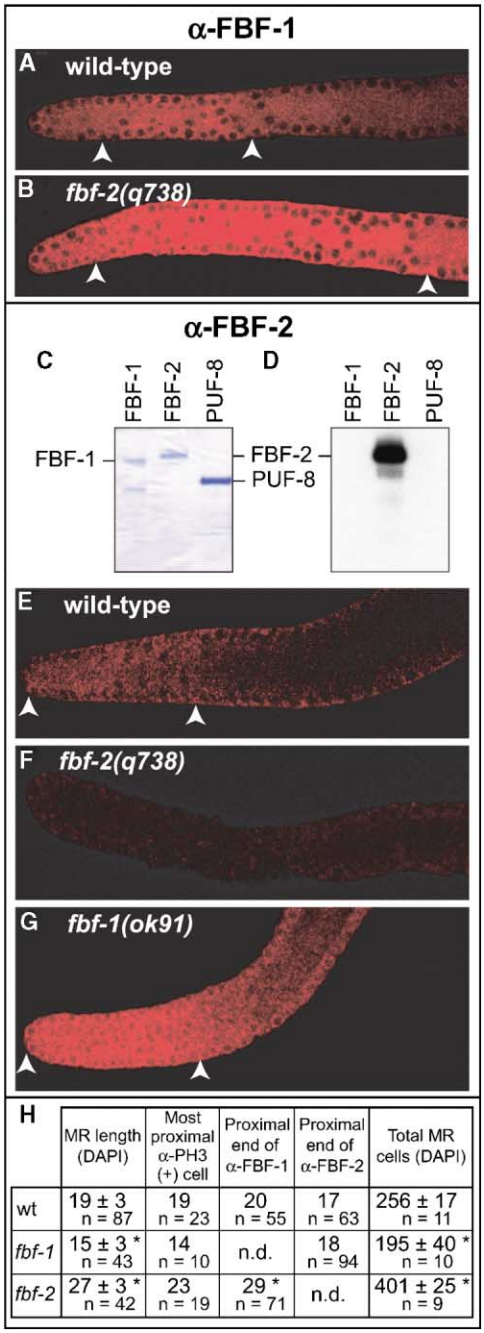

H

	MR length (DAPI)	Most proximal α-PH3 (+) cell	Proximal end of α-FBF-1	Proximal end of α-FBF-2	Total MR cells (DAPI)
wt	19 ± 3 n = 87	19 n = 23	20 n = 55	17 n = 63	256 ± 17 n = 11
fbf-1	15 ± 3 * n = 43	14 n = 10	n.d.	18 n = 94	195 ± 40 * n = 10
fbf-2	27 ± 3 * n = 42	23 n = 19	29 * n = 71	n.d.	401 ± 25 * n = 9

Figure 4. FBF-1 and FBF-2 Proteins Are Expressed in Distinct Patterns that Are Responsive to FBF Activity

(A, B, E–G) Extruded adult germlines, distal end is to left. Germlines were treated identically, and confocal images were taken with the same settings at the same magnification for comparison of (A) to (B) and of (E) and (F) to (G). White arrowheads highlight the distal and proximal boundaries of staining.

(A) FBF-1 staining in wild-type germline.

(B) FBF-1 increases in both extent and amount in *fbf-2(q738)* germlines.

(C and D) Replicate gels run with recombinant proteins: Coomassie-stained polyacrylamide gel (C) and Western blot with anti-FBF-2-specific antibodies (D).

(E) FBF-2 staining in wild-type germline.

(F) FBF-2 staining in *fbf-2(q738)* single mutant.

(G) FBF-2 increases in amount in *fbf-1(ok91)* single mutant germ lines, with respect to wild-type.

(H) Summary of effects of *fbf-1* and *fbf-2* mutations on mitotic region.

the epitope tag was not detectable by immunocytochemistry or Western analysis (B. Thompson and J.K., unpublished). We therefore abandoned this approach and asked instead if *fbf-2* expression could respond to a change in GLP-1 signaling.

To assay the *fbf* response to GLP-1 signaling, we stained for FBF-1 or FBF-2 after a shift of *glp-1(ts)* mutants to nonpermissive temperature. We included additional mutations to enhance the FBF signal and to decouple the response to GLP-1 signaling from the state of the cell. Therefore, these strains harbored three different types of mutations. First was *glp-1(q224ts)*, a mutation that abrogates GLP-1 signaling at 25°C, the restrictive temperature (Austin and Kimble, 1987). Second were *gld-1* and *gld-2*, which genetically transform the germline into a mitotic tumor (Kadyk and Kimble, 1998). Third was an *fbf-1* or *fbf-2* single mutant, which we included to increase the signal of FBF-2 or FBF-1 protein, respectively.

We first compared the abundance of FBF-1 protein in the presence of GLP-1 signaling (*gld-1 gld-2; fbf-2* mutants, n = 39) to that in the absence of GLP-1 signaling (*gld-1 gld-2; fbf-2; glp-1(ts)* mutants, n = 48) at 25°C. FBF-1 was uniformly distributed throughout the germline of each strain, and its level appeared the same (Figures 6E–6G). We then compared FBF-2 abundance in the presence and absence of GLP-1 signaling using similar strains (*gld-1 gld-2; fbf-1*, n = 25, and *gld-1 gld-2; fbf-1; glp-1(ts)* mutants, n = 26) at 25°C. In both strains, FBF-2 was present throughout the germline (Figures 6H and 6I). Therefore, FBF-2 cannot be wholly dependent on GLP-1 signaling, at least in these tumorous germlines. However, in those germlines with active GLP-1 signaling, FBF-2 was visibly higher in the distal region (Figure 6H, triangles) than in the rest of the germline (Figure 6H). In germlines without GLP-1 signaling, by contrast, FBF-2 was uniform (Figure 6I). To assess this apparent difference, we quantified FBF-2 staining (Figure 6J) and found that distal germ cells with wild-type GLP-1 signaling had about three times more FBF-2 than cells with defective GLP-1 signaling. We conclude that *fbf-2* responds to GLP-1 signaling.

fbf; glp-1 Mutants

The *glp-1* and *fbf-1 fbf-2* loss-of-function phenotypes are distinct: *glp-1* mutants have no stem cells at any stage of development, but *fbf-1 fbf-2* double mutants are defective only in adults. Furthermore, *fbf-2* single mutants are homozygous viable, with only minor defects in germline development (see above). Therefore, *fbf-2* is not likely to be the only target of GLP-1 signaling. Nonetheless, we considered the formal possibility that a change in *fbf* activity might bypass the need for GLP-1 signaling. To test this idea, we shifted *fbf-1; glp-1(ts)* and *fbf-2; glp-1(ts)* double mutants, as well as *fbf-1 fbf-2; glp-1(ts)* triple mutants, from permissive to restrictive temperature as early larval (L1), late larval (L4), or adult animals. In all cases, germ cells left the mitotic cell cycle and entered meiosis soon after the shift, abolishing

MR, mitotic region; n.d., no data. Distance from DTC scored in nuclei for MR length and proximal end of FBF staining. Asterisk indicates value is significantly different from wild-type ($p < 0.001$).

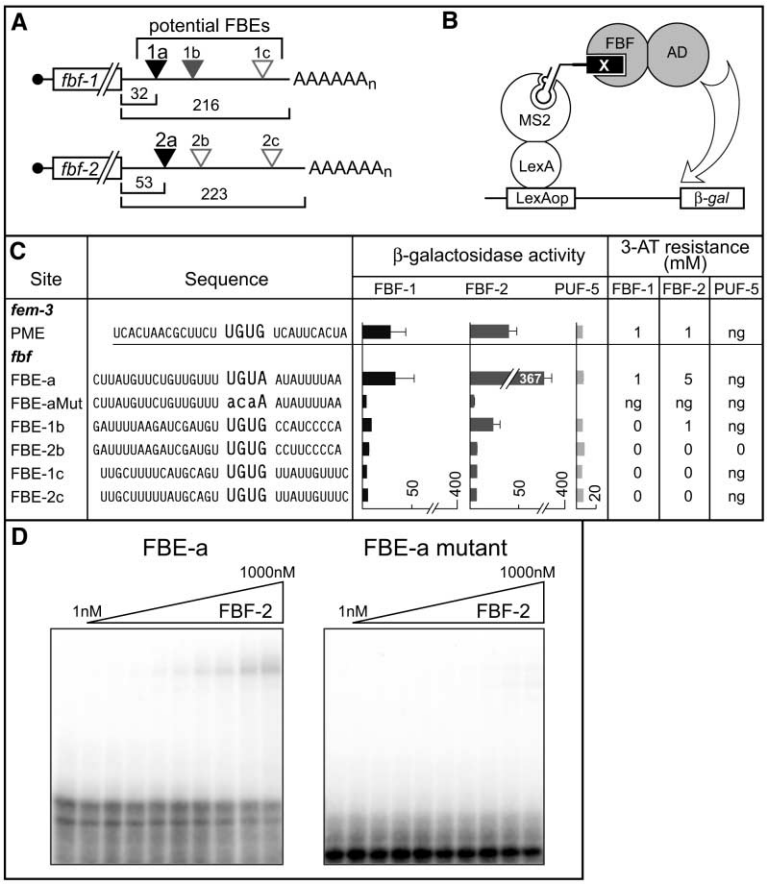

Figure 5. FBF-1 and FBF-2 Bind Specifically to Elements in Their 3′ Untranslated Regions

(A) Putative FBF binding elements in *fbf-1* and *fbf-2* 3′ UTRs; filled black triangles are elements that bind in vitro, gray triangle is the weak binding element, and white triangles are elements that do not bind in vitro. Numbers are nucleotide distance from the stop codon.

(B) The yeast three-hybrid system.

(C) Nucleotide sequence of predicted FBF binding elements and a mutated binding element (lower case) tested in the yeast three-hybrid system with FBF-1, FBF-2, and PUF-5 proteins. β-galactosidase activity is reported in relative light units and the highest concentration of 3-aminotriazole on which cells could grow is indicated; ng means that cells could not grow in the absence of histidine.

(D) Gel shifts. The FBE-a element interacts with FBF-2 in vitro; the "aca" change in the FBE-a mutant element abolishes the interaction with FBF-2.

germline proliferation during larval development and eliminating the mitotic region in adults. Therefore, GLP-1 signaling remains essential for promoting mitosis, even in the absence of *fbf-1* and *fbf-2*.

fbf Orthologs in the *C. briggsae* Genome

We identified probable *C. briggsae* orthologs of *fbf-1* and *fbf-2* by sequence comparisons. The *C. briggsae* genome encodes 12 PUF proteins (Supplemental Figure S1A at http://www.developmentalcell.com/cgi/content/full/7/5/697/DC1/). *C. briggsae* PUF-1 (CbPUF-1), CbPUF-2, and CbPUF-12 are more similar to each other than to any *C. elegans* PUF protein, suggesting that two duplication events occurred after the split between *C. briggsae* and *C. elegans*. Among *C. elegans puf* genes, *Cb-puf-1*, *Cb-puf-2*, and *Cb-puf-12* are most similar to *fbf-1* and *fbf-2* (Supplemental Figure S1A). Therefore, these two gene sets are likely to be derived from a common ancestor. Other *C. briggsae puf* genes are described in the legend to Supplemental Figure S1A.

The *C. briggsae puf-1*, *puf-2*, and *puf-12* genes share features with *fbf-1* and *fbf-2* (Supplemental Figures S1B–S1D). For example, *Cb-puf-2*, *Cb-puf-12*, and *Ce-fbf-2* all possess putative LAG-1 binding sites in their 5′ flanking regions. Conversely, *Cb-puf-1* and *Ce-fbf-1* lack putative LAG-1 binding sites in their 5′ flanking regions. Furthermore, *Cb-puf-1*, *Cb-puf-2*, and *Cb-puf-12* possess putative PUF binding sites in their putative 3′UTRs. Therefore, the common ancestor is likely to have been controlled by both Notch signaling and 3′UTR regulation. The paralogs are more similar than the orthologs, suggesting that the gene pairs were not derived from a duplicated ancestor. If true, then the genes within a pair may have evolved similar characters by convergent evolution. However, a more definitive analysis of the *C. briggsae* gene pair is necessary to make conclusions about the presence of regulatory binding sites as well as biological functions.

Discussion

fbf-1 and *fbf-2* Have Gene-Specific Effects on Patterning

FBF-1 and FBF-2 have two major roles in germline development: they promote mitotic divisions at the expense of meiosis and they promote oogenesis at the expense of spermatogenesis (Crittenden et al., 2002; Zhang et al., 1997). Previous studies suggested that these two nearly identical proteins are largely redundant. Whereas *fbf-1 fbf-2* double mutants lack germline mitoses and are sterile, most *fbf-1* null mutants are fertile (Crittenden et al., 2002). We find that most *fbf-2* single mutants are also fertile, confirming that FBF-1 or FBF-2 can compensate for each other and that both FBF proteins can direct mitosis and oogenesis.

Despite being interchangeable for fertility, *fbf-1* and

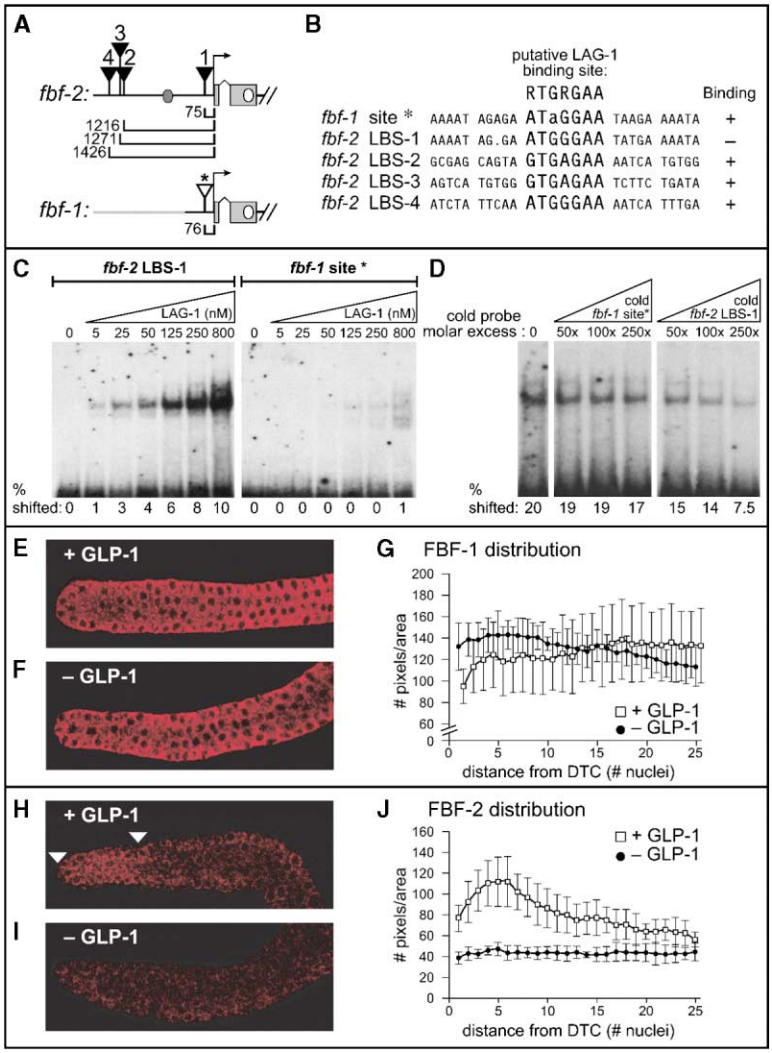

Figure 6. LAG-1 Binding Sites in the *fbf-2* 5′ Flanking Region

(A) Location of consensus LAG-1 binding sites (triangles) and motifs 1, 2 (ovals) in 5′ flanking region of *fbf-1* and *fbf-2*. White oval, motif 1 gray oval, motif 2. Numbers are nucleotide distance from the initiation codon. The sequence of the *fbf-1* and *fbf-2* 5′ flanking regions share no similarity (gray line) until ~350 bp upstream from the initiation codon.

(B) Sequences of putative LAG-1 binding sites with consensus at top. The 5′ flanking region of *fbf-1* does not contain a consensus LAG-1 binding site, though the 200 bp upstream of the predicted ATG are 91% identical in *fbf-1* and *fbf-2*. *fbf-1* site* sequence corresponds to site 1 in *fbf-2*.

(C) Gel retardation assay. The *fbf-2* probe interacts with the purified LAG-1. The *fbf-1* probe does not interact with LAG-1 in vitro.

(D) Gel retardation assay with unlabeled probe competition. The unlabeled *fbf-2* probe, but not the unlabeled *fbf-1* probe, competes with the ^{32}P-labeled *fbf-2* probe.

(E–J) FBF-2, but not FBF-1, is responsive to GLP-1 signaling. (E), (F), (H), and (I) extruded adult germlines, distal end to left. Germlines are mitotic throughout and have not entered meiosis due to genetic manipulation of cell fates. For comparison of (E) to (F) and of (H) to (I), germlines were treated identically and confocal images were taken with the same settings at the same magnification.

(E and F) FBF-1 levels are high and uniform throughout the tumorous *gld-2 gld-1; fbf-2* germline and the *gld-2 gld-1; fbf-2; glp-1(lf)* germline.

(G) Quantitation of FBF-1 staining in presence (square) or absence (solid circle) of GLP-1 signaling.

(H) FBF-2 levels increase in the distal region of the tumorous *gld-2 gld-1; fbf-1* germline (triangles highlight boundaries).

(I) FBF-2 levels are uniform in the absence of GLP-1 signaling in the *gld-2 gld-1; fbf-1; glp-1(lf)* germline. FBF-2 protein expression is responsive to GLP-1 signaling.

(J) Quantitation of FBF-2 staining in presence (square) or absence (solid circle) of GLP-1 signaling.

fbf-2 single mutants have opposing effects on the size of the mitotic region: the *fbf-1* mitotic region contains fewer cells than normal (Crittenden et al., 2002), but the *fbf-2* mitotic region has more cells than normal (this work). Because FBF-1 and FBF-2 have the same binding specificity in vitro (Crittenden et al., 2002; Eckmann et al., 2004; this work; Zhang et al., 1997) and the two *fbf* genes are largely interchangeable in vivo (Crittenden et al., 2002; this work), the genes are likely to be differentially regulated.

Two Controls of FBF Expression

The *fbf-2* gene is controlled, at least in part, by GLP-1/Notch signaling (Figure 7A). Several lines of evidence support this conclusion and suggest that the *fbf-2* control may be direct. First, the *fbf-2* 5′ flanking region possesses four LAG-1 binding sites. Second, both *fbf-2* mRNA and protein are localized to the distal germline, whereas *fbf-1* mRNA and protein are more broadly distributed. Third, FBF-2 abundance is reduced when GLP-1/Notch signaling is turned off, but FBF-1 appears unaffected. This last experiment was performed in a germline composed entirely of mitotic germ cells so that a difference in FBF level could not be attributed to a change in cell fate. Because *fbf-2* is expressed in germline tumors that lack GLP-1/Notch signaling, *fbf-2* transcription appears to rely on both GLP-1-dependent and GLP-1-independent mechanisms.

The *fbf-2* activation by GLP-1/Notch signaling forges the first link between two major mechanisms that regulate germline mitoses (Figure 7A). Nonetheless, GLP-1/Notch signaling must have other target genes relevant to germline mitoses, because signaling remains essential in *fbf-2* and *fbf-1 fbf-2* mutants. We therefore propose the existence of other target genes that influence germline mitoses (Figure 7A, gene X).

A second control limits FBF abundance by autoregulation: FBF-1 increases in *fbf-2* single mutants, and vice versa (Figure 7B). This reciprocal repression appears to be direct: the *fbf-1* and *fbf-2* 3′ UTRs contain an FBF

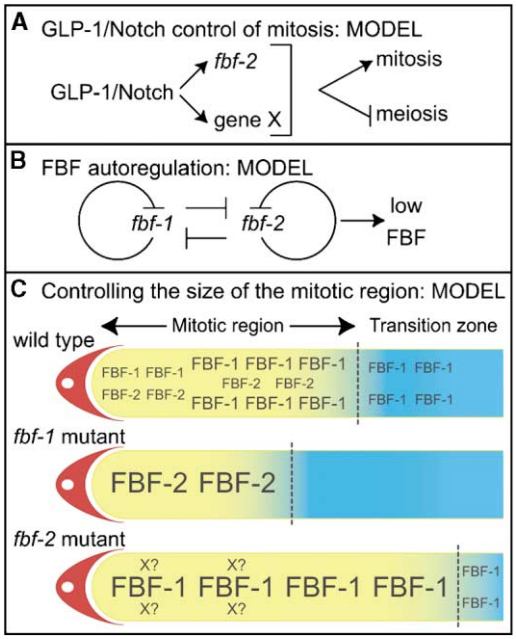

Figure 7. Models for FBF-1 and FBF-2 Regulation and for the Control of the Mitotic Region

(A) GLP-1 activates *fbf-2* transcription to promote germline mitoses. GLP-1 is also likely to activate other genes (gene X) for the same purpose.

(B) FBF autoregulation maintains a low level of FBF.

(C) Top, wild-type germline with combined FBF-1 and FBF-2 in the mitotic region; middle, *fbf-1* mutant germline with FBF-2 dominating in a shorter than normal mitotic region; bottom, *fbf-2* mutant germline with FBF-1 dominating in an expanded mitotic region.

binding element (FBE). A simple model is that FBF-1 and FBF-2 bind and downregulate the expression of both *fbf-1* and *fbf-2* mRNAs. Although in vivo evidence supports only crossregulation (e.g., FBF-1 represses *fbf-2* expression), it seems likely that FBF-1 and FBF-2 also control their own mRNAs. We suggest that FBF autoregulation provides a critical mechanism for controlling FBF-1 and FBF-2 at their normal steady-state levels in wild-type animals, although other molecular mechanisms may also impact FBF abundance (e.g., feedback regulation by other regulators).

FBF and Size of the Mitotic Region

The *fbf-1* and *fbf-2* genes are crucial regulators of the size of the mitotic region. As such, these genes control the size of a developmental field (i.e., the mitotic region) and the average number of cells within that field. In wild-type germlines, FBF distribution includes both FBF-1 and FBF-2 (Figure 7C, top), both kept at relatively low levels by FBF autoregulation. In *fbf-1* mutants, FBF-2 protein is more abundant than wild-type but remains restricted to the distal germline (Figures 4G and 7C, middle). That distal localization is likely to reflect *fbf-2* regulation by GLP-1/Notch signaling from the DTC. As a consequence, the *fbf-1* mutant mitotic region is shorter in length along the distal-proximal axis than wild-type, and there are fewer mitotic cells. In *fbf-2* mutants, FBF-1 protein is both more abundant and more broadly distributed (Figures 4B and 7C, bottom). The *fbf-2* mitotic region is correspondingly longer in length and possesses more cells than wild-type. Therefore, in each case, mitotic region size corresponds remarkably well with the extent of FBF.

FBF is part of a regulatory network that controls the mitosis/meiosis decision and size of the mitotic region (Crittenden et al., 2003). Other network components also affect mitotic region size; for example, *gld-2* and *gld-3* normally promote entry into meiosis, and animals lacking either gene have a larger than normal mitotic region (Eckmann et al., 2004). The GLD-3 protein interferes with FBF binding to its target mRNAs (Eckmann et al., 2002), suggesting that GLD-3 may affect mitotic region size, at least in part, by antagonizing FBF. The *gld-1* and *nos-3* genes also promote meiosis but are in a regulatory branch that is redundant with the *gld-2*/*gld-3* branch (Eckmann et al., 2004; Hansen et al., 2004; Jones et al., 1996; Kadyk and Kimble, 1998). An analysis of the interplay among all regulators in this network is beyond the scope of this work, but it is an important challenge for the future.

fbf-1 and *fbf-2*: Implications for Evolution and Development

Gene duplications can provide the raw material for evolution of genomic diversity (Ohno, 1970). Many duplicated genes become functionally divergent (e.g., Carroll et al., 2001), and *fbf-1* and *fbf-2* have much in common with them. For example, the *fbf* genes have acquired distinct *cis*-acting regulatory regions, a well-known mechanism for divergence of duplicated genes (e.g., Ohta, 2003; Rudel and Kimble, 2001).

Duplicated genes are preserved when each member of the pair loses distinct functions or regulatory elements, a process known as subfunctionalization (Lynch and Force, 2000). Consistent with this process, FBF-2 appears specialized for response to GLP-1/Notch signaling, and FBF-1, perhaps, for expansion of the mitotic region beyond the sphere of GLP-1/Notch influence. It is intriguing that the most similar *fbf* orthologs in *C. briggsae* are also associated with putative LAG-1 binding sites as well as putative PUF regulatory elements. Therefore, their common ancestor was probably controlled by both Notch signaling and 3′ UTR repression.

The abundance of many key developmental regulators is carefully controlled, and 2-fold changes can be deleterious. Most relevant to this discussion are cases in which a 2-fold increase is harmful (Bardoni et al., 1994; Chial et al., 1999; Huang et al., 1999; Jordan et al., 2001; Papp et al., 2003; Schedl et al., 1996). We suggest that genes subject to negative autoregulation may be more able to escape dosage problems, permitting their duplicates to persist long enough for subfunctionalization and fixation. In keeping with this idea, reciprocal repression or antagonism has been observed for many duplicated gene pairs (e.g., Pax-6/Pax-2; Schwartz et al., 2000; this work).

What selective pressures might the duplicated *fbf* genes face? Mutant *C. elegans* hermaphrodites with either fewer or more than the normal number of sperm

cannot compete with hermaphrodites making the wild-type number of sperm (Hodgkin and Barnes, 1991). Therefore, regulators of the sperm/oocyte decision must be under strong selection to produce an optimal number of hermaphrodite sperm before switching to oogenesis. We do not know if similar selective forces act on controls of mitotic region size.

The *fbf* reciprocal repression is actually a subnetwork within the larger regulatory network controlling mitosis/meiosis and sperm/oocyte decisions (Crittenden et al., 2003; Eckmann et al., 2004; Hansen et al., 2004). We propose that this *fbf* subnetwork enables a more precise control over patterning in the germline and that *fbf-1* and *fbf-2* provide a paradigm for how duplicated genes can diverge to fine-tune patterning during animal development.

Experimental Procedures

Nematode Strains

All strains were derivatives of Bristol strain N2 and grown by standard procedures at 20°C unless specified (Brenner, 1974). Mutations include *LG II*: *fbf-1(ok91, ok224)* (Crittenden et al., 2002); and *fbf-2(q655, q735, q738)* (this work); *fbf* mutations were balanced with *mnIn1[mIs14 dpy-10(e128)]*; *LG III*: *glp-1(q224ts)* (Austin and Kimble, 1987; Kodoyianni et al., 1992). *fbf-2* deletions were generated by ethyl methane sulfonate mutagenesis, isolated in a PCR-based screen (Kraemer et al., 1999), and out-crossed at least eight times. RNA products in deletion mutants were confirmed by RT-PCR and subsequent sequencing, all by standard procedures (Sibley et al., 1993).

fbf-1(ok91); glp-1(ts), *fbf-2(q738); glp-1(ts)* and *fbf-1(ok91) fbf-2(q704)/mnIn1[mIs14 dpy-10(e128)]; glp-1(ts)* strains were maintained at 15° and progeny examined after a shift to 25°C.

Assessing Size of Mitotic Region and Number of Hermaphrodite Sperm

Dissected adult germlines (~24 hr past mid-L4) were DAPI (4′,6-diamidino-2-phenylindole)-stained by standard techniques (Crittenden and Kimble, 1998) to examine nuclear morphology. Most nuclei in the mitotic region are round (interphase) or condensed (metaphase), whereas most in the transition zone are crescent-shaped (Dernburg et al., 1998). The boundary between mitotic region and transition zone corresponds to the position along the distal-proximal axis (measured in number of nuclei) at which most nuclei are crescent-shaped. Germlines were also stained with anti-PH3 antibodies (Hendzel et al., 1997), anti-GLP-1 (Crittenden et al., 1994), anti-REC-8 (Pasierbek et al., 2001), and anti-HIM-3 (Zetka et al., 1999) to confirm mitotic region size.

In Situ Hybridization, Immunocytochemistry, and Western Blots

For in situ hybridization, young adult germlines were extruded and stained by standard procedures (Jones et al., 1996). To generate FBF-2 antibodies, rabbits were injected with keyhole-limpet-hemocyanin-coupled peptides corresponding to FBF-2 amino acids 606–632 (Genemed Synthesis, Inc). Affinity-purified antibodies (diluted 1:5) were preincubated with acetone powder derived from *fbf-2(q655)* animals to reduce nonspecific staining (Epstein and Shakes, 1995). Extruded germlines were fixed in −20°C methanol, followed by −20°C acetone (Crittenden and Kimble, 1998).

Germlines were stained with rat anti-FBF-1 (1:7), rabbit anti-FBF-2 (1:5), and rat anti-GLP-1 antibodies (1:5), according to standard procedures (Crittenden et al., 1994). The nuclear pore-specific antibody, Mab-414 (Covance/BABCO, 1:400), served as control, and DAPI was used to visualize DNA. Epifluorescent images were captured with a Zeiss Axioskop equipped with a Hamamatsu digital CCD camera, and they were processed with the program Openlab 3.1.7. Confocal images were collected on a Bio-Rad MRC1024 confocal microscope. Fluorescence was quantified using NIH ImageJ software. Western blots were performed with in vitro transcription/translation products from rabbit reticulocyte lysate (Promega) and purified GST-FBF-1, GST-FBF-2, and GST-PUF-8 from bacterial lysates.

Analysis of FBF Binding Elements

Candidate FBF binding sites were identified in *fbf-1* and *fbf-2* 3′ UTR sequences using optimal sequences deduced from comparisons of natural FBF targets as well as mutagenesis of known sites (D.B., B. Hook, A. Hajarnavis, L. Opperman, R. Durbin, and M.W., unpublished data). Three-hybrid assays were performed as described (Bernstein et al., 2002). DNA oligonucleotides were designed to contain the predicted FBE and cloned into pIIIA/MS2-2 vector. Gal4 activation domain fusion proteins with FBF-1 (amino acids 121–614), FBF-2 (amino acids 121–634), or PUF-5 (amino acids 1–553) were expressed from pACT2 plasmids. β-galactosidase was quantified using the Beta-Glo system (Promega) after normalizing for cell number; *HIS3* activation was monitored by plating cells on increasing concentrations of 3-aminotriazole (3-AT), a competitive inhibitor of the His3p enzyme.

Gel Retardation Assays

GST-FBF-2 (amino acids 121–634) and GST-LAG-1 (amino acids 48–673) were expressed in bacteria, purified on Glutathione Sepharose 4B beads, and cleaved from beads with PreScission Protease (Amersham). For RNA/FBF-2 interaction studies, 0–1000 nM FBF-2 protein was combined with 100 fMol ^{32}P-end-labeled RNA oligoribonucleotides (IDT) identical to the *fbf-1* FBE-a and FBE-aMut (Figure 5C). Protein and RNA were incubated at room temperature for 30 min in 10 mM HEPES (pH 7.4), 1 mM EDTA, 2 μg yeast tRNA (Sigma), 50 mM KCl, 2 mM DTT, and 0.02% Tween-20.

For DNA/LAG-1 binding studies, purified LAG-1 (0–800 nM) was added to each reaction. 50 fmol ^{32}P-end-labeled double-stranded DNA probe was incubated with the LAG-1 and buffers as described (Zimber-Strobl et al., 1994). For competition assays, 5–25 pmol unlabeled dsDNA probe was combined with the 50 fmol ^{32}P-end-labeled double-stranded DNA probe, and 3 pmol purified LAG-1 was added to each reaction.

C. briggsae, *C. elegans* Genomic Sequence Comparison

A BLAST search of the *C. briggsae* genome assembly eb25.agp8 identified sequences with high similarity to *C. elegans* PUF proteins. A Hidden Markov Model search using the model presented in Wickens et al. (2002) was used to identify the PUF domain of each *C. briggsae* protein. The domains were aligned and a heuristic tree created using the PAUP program suite in GCG (Wisconsin Package, Version 10.3). The tree was visualized using njplot (Perrière and Gouy, 1996).

Acknowledgments

We are grateful to A. Fire, P. Pasierbek, and M. Zetka for reagents and members of the Kimble and Wickens laboratories for helpful discussions during the course of this work. We thank Peggy Kroll-Conner, Carolyn Stroncek, and Gary Molder for assistance with generating *fbf-2* deletion mutants, Brad Hook for purified FBF-2 protein and expertise in its analysis, and Kelley Harris for help with characterization of *fbf-2(q735)*. We thank Anne Helsley-Marchbanks, Laura Vanderploeg, and Robin Davies for help with preparing the manuscript and figures. We also thank Eric Haag and Alana Doty for advice on *C. briggsae puf* genes. L.B.L. was supported by National Institutes of Health Predoctoral Training Grant T32 GM07215 in Molecular Biosciences and J.K. is an investigator with the Howard Hughes Medical Institute (HHMI).

Received: June 28, 2004
Revised: August 3, 2004
Accepted: August 30, 2004
Published: November 8, 2004

References

Austin, J., and Kimble, J. (1987). *glp-1* is required in the germ line for regulation of the decision between mitosis and meiosis in *C. elegans*. Cell *51*, 589–599.

Bardoni, B., Zanaria, E., Guioli, S., Floridia, G., Worley, K.C., Tonini, G., Ferrante, E., Chiumello, G., McCabe, E.R., Fraccaro, M., et al. (1994). A dosage sensitive locus at chromosome Xp21 is involved in male to female sex reversal. Nat. Genet. *7*, 497–501.

Bernstein, D.S., Buter, N., Stumpf, C., and Wickens, M. (2002). Analyzing mRNA-protein complexes using a yeast three-hybrid system: methods and applications. Methods *26*, 123–141.

Berset, T., Fröhli Hoier, E., Battu, G., Canevascini, S., and Hajnal, A. (2001). NOTCH inhibition of RAS signaling through MAP kinase phosphatase LIP-1 during *C. elegans* vulval development. Science *291*, 1055–1058.

Brenner, S. (1974). The genetics of *Caenorhabditis elegans*. Genetics *77*, 71–94.

Carles, C.C., and Fletcher, J.C. (2003). Shoot apical meristem maintenance: the art of a dynamic balance. Trends Plant Sci. *8*, 394–401.

Carroll, S., Grenier, J.K., and Weatherbee, S.D. (2001). From DNA to Diversity: Molecular Genetics and the Evolution of Animal Design (Malden, MA: Blackwell Science).

Chial, H.J., Giddings, T.H., Jr., Siewert, E.A., Hoyt, M.A., and Winey, M. (1999). Altered dosage of the *Saccharomyces cerevisiae* spindle pole body duplication gene, *NDC1*, leads to aneuploidy and polyploidy. Proc. Natl. Acad. Sci. USA *96*, 10200–10205.

Christensen, S., Kodoyianni, V., Bosenberg, M., Friedman, L., and Kimble, J. (1996). *lag-1*, a gene required for *lin-12* and *glp-1* signaling in *Caenorhabditis elegans*, is homologous to human CBF1 and *Drosophila* Su(H). Development *122*, 1373–1383.

Crittenden, S., and Kimble, J. (1998). Confocal methods for *Caenorhabditis elegans*. In Methods in Molecular Biology, Vol. 122: Confocal Microscopy Methods and Protocols, S. Paddock, ed. (Totowa, NJ: Humana Press, Inc.), pp. 141–151.

Crittenden, S.L., Troemel, E.R., Evans, T.C., and Kimble, J. (1994). GLP-1 is localized to the mitotic region of the *C. elegans* germ line. Development *120*, 2901–2911.

Crittenden, S.L., Bernstein, D.S., Bachorik, J.L., Thompson, B.E., Gallegos, M., Petcherski, A.G., Moulder, G., Barstead, R., Wickens, M., and Kimble, J. (2002). A conserved RNA-binding protein controls germline stem cells in *Caenorhabditis elegans*. Nature *417*, 660–663.

Crittenden, S.L., Eckmann, C.R., Wang, L., Bernstein, D.S., Wickens, M., and Kimble, J. (2003). Regulation of the mitosis/meiosis decision in the *Caenorhabditis elegans* germline. Philos. Trans. R. Soc. Lond. B Biol. Sci. *358*, 1359–1362.

Dernburg, A.F., McDonald, K., Moulder, G., Barstead, R., Dresser, M., and Villeneuve, A.M. (1998). Meiotic recombination in *C. elegans* initiates by a conserved mechanism and is dispensable for homologous chromosome synapsis. Cell *94*, 387–398.

Eckmann, C.R., Kraemer, B., Wickens, M., and Kimble, J. (2002). GLD-3, a Bicaudal-C homolog that inhibits FBF to control germline sex determination in *C. elegans*. Dev. Cell *3*, 697–710.

Eckmann, C.R., Crittenden, S.L., Suh, N., and Kimble, J. (2004). GLD-3 and control of the mitosis/meiosis decision in the *C. elegans* germ line. Genetics, in press.

Epstein, H.F., and Shakes, D.C. eds. (1995). *Caenorhabditis elegans*: Modern Biological Analysis of an Organism (New York: Academic Press, Inc.).

Fuchs, E., Tumbar, T., and Guasch, G. (2004). Socializing with the neighbors: stem cells and their niche. Cell *116*, 769–778.

Hansen, D., Wilson-Berry, L., Dang, T., and Schedl, T. (2004). Control of the proliferation versus meiotic development decision in the *C. elegans* germline through regulation of GLD-1 protein accumulation. Development *131*, 93–104.

Hendzel, M.J., Wei, Y., Mancini, M.A., Van Hooser, A., Ranalli, T., Brinkley, B.R., Bazett-Jones, D.P., and Allis, C.D. (1997). Mitosis-specific phosphorylation of histone H3 initiates primarily within pericentromeric heterochromatin during G2 and spreads in an ordered fashion coincident with mitotic chromosome condensation. Chromosoma *106*, 348–360.

Hodgkin, J., and Barnes, T.M. (1991). More is not better: brood size and population growth in a self-fertilizing nematode. Proc. R. Soc. Lond. B. Biol. Sci. *246*, 19–24.

Huang, B., Wang, S., Ning, Y., Lamb, A.N., and Bartley, J. (1999). Autosomal XX sex reversal caused by duplication of SOX9. Am. J. Med. Genet. *87*, 349–353.

Jones, A.R., Francis, R., and Schedl, T. (1996). GLD-1, a cytoplasmic protein essential for oocyte differentiation, shows stage-and sex-specific expression during *Caenorhabditis elegans* germline development. Dev. Biol. *180*, 165–183.

Jordan, B.K., Mohammed, M., Ching, S.T., Délot, E., Chen, X.-N., Dewing, P., Swain, A., Rao, P.N., Elejalde, B.R., and Vilain, E. (2001). Up-regulation of WNT-4 signaling and dosage-sensitive sex reversal in humans. Am. J. Hum. Genet. *68*, 1102–1109.

Kadyk, L.C., and Kimble, J. (1998). Genetic regulation of entry into meiosis in *Caenorhabditis elegans*. Development *125*, 1803–1813.

Kodoyianni, V., Maine, E.M., and Kimble, J. (1992). Molecular basis of loss-of-function mutations in the *glp-1* gene of *Caenorhabditis elegans*. Mol. Biol. Cell *3*, 1199–1213.

Kraemer, B., Crittenden, S., Gallegos, M., Moulder, G., Barstead, R., Kimble, J., and Wickens, M. (1999). NANOS-3 and FBF proteins physically interact to control the sperm-oocyte switch in *Caenorhabditis elegans*. Curr. Biol. *9*, 1009–1018.

Lynch, M., and Force, A. (2000). The probability of duplicate gene preservation by subfunctionalization. Genetics *154*, 459–473.

Murata, Y., and Wharton, R. (1995). Binding of Pumilio to maternal *hunchback* mRNA is required for posterior patterning in *Drosophila* embryos. Cell *80*, 747–756.

Ohno, S. (1970). Evolution by Gene Duplication (Heidelberg, Germany: Springer-Verlag).

Ohta, T. (2003). Evolution by gene duplication revisited: differentiation of regulatory elements versus proteins. Genetica *118*, 209–216.

Papp, B., Pál, C., and Hurst, L.D. (2003). Dosage sensitivity and the evolution of gene families in yeast. Nature *424*, 194–197.

Pasierbek, P., Jantsch, M., Melcher, M., Schleiffer, A., Schweizer, D., and Loidl, J. (2001). A *Caenorhabditis elegans* cohesion protein with functions in meiotic chromosome pairing and disjunction. Genes Dev. *15*, 1349–1360.

Perrière, G., and Gouy, M. (1996). WWW-Query: an on-line retrieval system for biological sequence banks. Biochimie *78*, 364–369.

Pourquié, O. (2003). Vertebrate somitogenesis: a novel paradigm for animal segmentation? Int. J. Dev. Biol. *47*, 597–603.

Rudel, D., and Kimble, J. (2001). Conservation of *glp-1* regulation and function in nematodes. Genetics *157*, 639–654.

Schedl, A., Ross, A., Lee, M., Engelkamp, D., Rashbass, P., van Heyningen, V., and Hastie, N.D. (1996). Influence of PAX6 gene dosage on development: overexpression causes severe eye abnormalities. Cell *86*, 71–82.

Schwartz, M., Cecconi, F., Bernier, G., Andrejewski, N., Kammandel, B., Wagner, M., and Gruss, P. (2000). Spatial specification of mammalian eye territories by reciprocal transcriptonal repression of Pax2 and Pax6. Development *127*, 4325–4334.

SenGupta, D.J., Zhang, B., Kraemer, B., Pochart, P., Fields, S., and Wickens, M. (1996). A three-hybrid system to detect RNA-protein interactions *in vivo*. Proc. Natl. Acad. Sci. USA *93*, 8496–8501.

Sibley, M.H., Johnson, J.J., Mello, C.C., and Kramer, J.M. (1993). Genetic identification, sequence, and alternative splicing of the *Caenorhabditis elegans* α2(IV) collagen gene. J. Cell Biol. *123*, 255–264.

Tadauchi, T., Matsumoto, K., Herskowitz, I., and Irie, K. (2001). Post-transcriptional regulation through the HO 3′-UTR by Mpt5, a yeast homolog of Pumilio and FBF. EMBO J. *20*, 552–561.

Tickle, C. (2003). Patterning systems—from one end of the limb to the other. Dev. Cell *4*, 449–458.

Wickens, M., Bernstein, D.S., Kimble, J., and Parker, R. (2002). A PUF family portrait: 3′UTR regulation as a way of life. Trends Genet. *18*, 150–157.

Yoo, A.S., Bais, C., and Greenwald, I. (2004). Crosstalk between the EGFR and LIN-12/Notch pathways in *C. elegans* vulval development. Science *303*, 663–666.

Yu, H., Yoo, A.S., and Greenwald, I. (2004). Cluster analyzer for

transcription sites (CATS): a C++-based program for identifying clustered transcription factor binding sites. Bioinformatics *20*, 1198–1200.

Zetka, M.C., Kawasaki, I., Strome, S., and Müller, F. (1999). Synapsis and chiasma formation in *Caenorhabditis elegans* require HIM-3, a meiotic chromosome core component that functions in chromosome segregation. Genes Dev. *13*, 2258–2270.

Zhang, B., Gallegos, M., Puoti, A., Durkin, E., Fields, S., Kimble, J., and Wickens, M.P. (1997). A conserved RNA-binding protein that regulates sexual fates in the *C. elegans* hermaphrodite germ line. Nature *390*, 477–484.

Zimber-Strobl, U., Stroble, L.J., Meitinger, C., Hinrichs, R., Sakai, T., Furukawa, T., Honjo, T., and Bornkamm, G.W. (1994). Epstein-Barr virus nuclear antigen 2 exerts its transactivating function through interaction with recombination signal binding protein RBP-J_K, the homologue of *Drosophila Suppressor of Hairless*. EMBO J. *13*, 4973–4982.